Theoret. Chim. Acta (Berl.) 40, 33–45 (1975)

Localized Molecular Orbitals for Polyatomic Molecules.
III. Monocyclic Aromatic Rings

Daniel A. Kleier, David A. Dixon and William N. Lipscomb
Department of Chemistry, Harvard University

Received June 13, 1975

Molecular wavefunctions have been generated by the PRDDO (Partial Retention of Diatomic Differential Overlap) method for the monocyclic aromatic rings containing six π-electrons ($C_4H_4^{-2}$, $C_5H_5^-$, C_6H_6, $C_7H_7^+$, and $C_8H_8^{+2}$) and ten π-electron species ($C_8H_8^{-2}$, $C_9H_9^-$, $C_{10}H_{10}$). The eigenvalue spectra of the canonical molecular orbitals are presented. Localized molecular orbitals (LMO's) generated using the Boys criterion are reported for localizations involving all occupied molecular orbitals (complete localizations) and localizations of the π orbitals only. We find evidence for σ-π separation in the complete localizations for some of these molecules even though the Boys criterion is often biased against such results. We demonstrate for C_6H_6 and find for the other molecules that the π-orbital localizations are indeterminate (i.e. there are an infinite number of equally satisfactory LMO structures between two limiting extremes). This result may be viewed as a corollary of Hückel's $(4n+2)$ rule for aromaticity.

Key words: Aromatic rings – Localized molecular orbitals – Partial retention of diatomic differential overlap

1. Introduction

Localized molecular orbitals (LMO's), which are useful for studies of chemical bonding, are especially interesting in comparisons within a homologous series of molecules [1]. Here we generate and compare the LMO's for a series of monocyclic aromatic hydrocarbons. These LMO's are generated from canonical molecular orbitals (CMO's) by a unitary transformation which leaves invariant both the total energy and the total electronic density. This unitary transformation can be based on a number of internal criteria, for example, the Edmiston-Ruedenberg (ER) criterion [2], or that of Boys [3, 4]. Except for a few well-noted differences [4], these two criteria yield quantitatively similar results, and we use the latter criterion here because it is computationally much more efficient.

Previously we have primarily used LMO's to study the bonding in the boron hydrides and carboranes [1, 5]. Recently, we have determined the LMO's by this Boys criterion for a number of fused polycyclic aromatic ring systems [6], for the amino acids [7] (containing first row atoms only) and for some heterocyclic ring systems [8]. In the course of this work we decided to determine the LMO's, described here, for the monocyclic aromatic systems having four to ten carbon atoms. We discuss the complete (all occupied orbital) localizations and compare these to the π-orbital localizations. We shall see that the delocalized nature of the

Table 1. Molecular energies and the benzene ionization potentials

A. Molecule	Energy (a.u.)
$C_4H_4^{-2}$	−152.821
$C_5H_5^-$	−191.849
C_6H_6	−230.356
$C_7H_7^+$	−268.481
$C_8H_8^{-2}$	−306.688
$C_9H_9^-$	−345.349
$C_{10}H_{10}$	−383.695

B. Benzene Orbital Ionization Potentials[a]

Orbital	PRDDO	SCF[b]	Experiment[c]
$E\pi$	9.26	7.99	9.3
$E\sigma$	13.51	12.03	11.4
$A\pi$	13.92	12.72	12.1

[a] Ionization potentials are given in eV and are calculated as the negative of the orbital eigenvalue according to Koopmans' Theorem.

[b] Ref. [11a].

[c] Ref. [11b].

π electrons in these systems is reflected by the indeterminacy of the π-only localizations as judged by the second derivative test [4, 9]. We demonstrate that this is a necessary consequence of the symmetry of the occupied π-CMO's.

2. Results of the SCF Calculation

SCF calculations were done using the PRDDO method [10] which is an all electron approximate *ab initio* method using a minimum basis set of Slater orbitals. Standard Slater exponents were used for carbon while the 1*s* exponent on hydrogen was set at 1.2. The $C_nH_n(n=4\text{–}10)$ molecular geometries were taken as regular *n*-gons with sides of 1.40 Å and C–H bond distances of 1.08 Å. The molecules are shown in Fig. 2.

Total energies for these molecules are presented in Table 1 while the π-eigenvalue spectrum is shown in Fig. 1. For molecules with bound orbital eigenvalues, the negative of the eigenvalue corresponds to the ionization potential as estimated by Koopmans' theorem. The ionization potentials for benzene from experiment and from *ab initio* minimum basis set SCF calculations [11] are in Table 1B for comparison with our values. Both are in reasonable agreement with PRDDO values. From the plot of eigenvalue versus ring size a marked trend can be noted for both the six and ten π electron series. The eigenvalues become more negative as the ionic charge goes from negative to positive. In fact, $C_4H_4^{-2}$ has no negative π eigenvalues while in $C_8H_8^{+2}$ the upper π orbital is bound by more than 20 eV. For $C_8H_8^{-2}$ a mixture of bound and unbound π levels exists suggesting (as is found in the large boron hydrides [12]) that a large number of centers will tend to stabilize excess negative charge.

The other important feature of the eigenvalue spectrum is the amount of σ-π interleaving. Consistent with experimental measurements [11a], we find that the $A\pi$ orbital of benzene is below the $E\sigma$ orbital. For $C_4H_4^{-2}$ and $C_7H_7^+$, we find

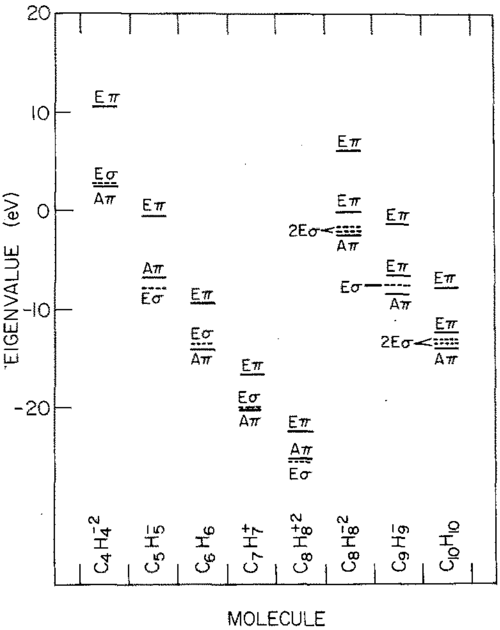

Fig. 1. Eigenvalue spectra (eV) of the monocyclic aromatic rings arranged according to size. Solid lines are π eigenvalues and dashed lines are σ eigenvalues. The negative of the eigenvalue for bound orbitals is the ionization potential as given by Koopmans' theorem

a similar result while for $C_5H_5^-$ and $C_8H_8^{+2}$ there is no interleaving. For $C_5H_5^-$ the absence of interleaving is more apparent than in $C_8H_8^{+2}$ where the $E\sigma$ and $E\pi$ are almost degenerate. The nonionic ten electron molecule $C_{10}H_{10}$ shows an interleaving similar to that of C_6H_6. The two sets of $E\pi$ orbitals are separated from the $A\pi$ orbital by two sets of $E\sigma$ orbitals. We find this same result for $C_8H_8^{-2}$ but for $C_9H_9^-$ we find only one set of $E\sigma$ orbitals interleaving the $E\pi$ and $A\pi$ levels.

3. Localized Molecular Orbitals: Theory

The LMO's for the molecules in this paper are shown in Fig. 2. The LMO's were calculated using the Boys criterion [3] and the 2×2 procedure suggested by Edmiston and Ruedenberg [2] as described in Ref. 4. In column A we show the complete localization results[1] and in columns B and C we present the π-only LMO's. The SOS[2] and eigenvalues of the second derivative test[3] are shown in Table 2. Before we discuss the LMO results for individual molecules, we present

---

[1] Complete localization refers to localizations which seek to maximize the sum of squares (see footnote 2) by transforming all of the occupied MO's. The LMO's so derived are called complete LMO's. The π-only localizations are those where only occupied π orbitals are included in the localization giving π-LMO's.

[2] SOS is the acronym for sum of squared centroid distances and is given by $\text{SOS} = \sum_{\text{occ}} \bar{r}_{ii}^2$ where $\bar{r}_{ii}$ is the centroid of the ith MO relative to some arbitrary origin.

[3] The most positive eigenvalues, $v_{\max}$, of the second derivative matrix (Ref. 4) are presented in Table 2. If the most positive eigenvalue is negative, a maximum has been reached. A zero value of $v_{\max}$ suggests a plateau or flat maximum.

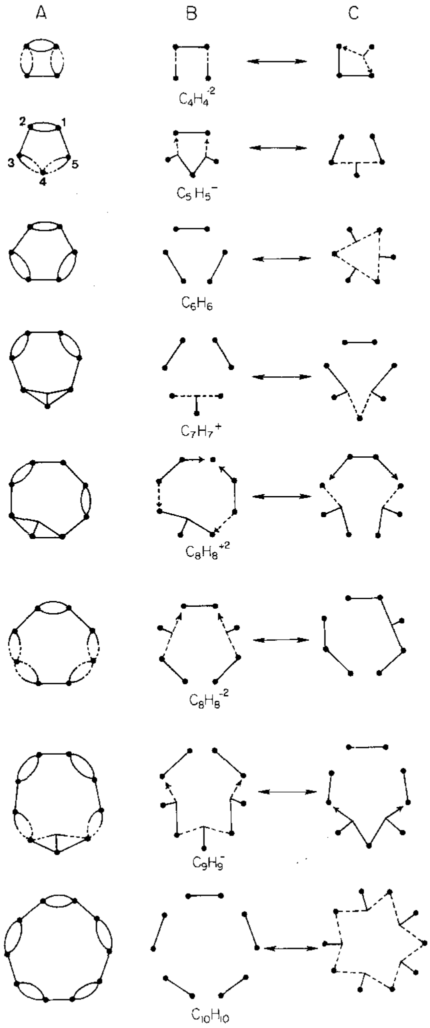

Fig. 2. Bonding patterns for the localized molecular orbitals (LMO's). Column A. LMO's for the complete localization (complete LMO's). Columns B and C depict limiting structures from the π-electron localizations. The LMO structures in column B are those which most closely resemble those in column A. The conventions for drawing these representations are given in Ref. 1 except that we have also indicated the polarity of the τ bonds in column A by drawing the bond solid to the centers with the higher electron populations and dashed to the centers with lower population. The polarized bonds insure the electroneutrality and equivalence of the carbons within each of these structures

a discussion of the SOS surface corresponding to the π orbitals of benzene.

The occupied π CMO's of benzene transform according to the A_{2u} and E_{1g} representations of the D_{6h} point group:

$$\begin{aligned}\psi(A_{2u}) &= N_{A_{2u}}(\phi_1+\phi_2+\phi_3+\phi_4+\phi_5+\phi_6)\\ \psi(E_{1gy}) &= N_{E_{1gy}}(2\phi_1+\phi_2-\phi_3-2\phi_4-\phi_5+\phi_6)\\ \psi(E_{1gx}) &= N_{E_{1gx}}(\phi_2+\phi_3-\phi_5-\phi_6)\end{aligned} \tag{1}$$

Table 2. Boys localization results for complete and π-only localizations

Molecule	SOS (complete)[a]	v^{b}_{max}(complete)	SOS(π)[a]	$v^{b}_{max}(\pi)$
$C_4H_4^{-2}$	77.243	−1.33	5.016	0.00
$C_5H_5^-$	120.300	−0.66	6.920	0.00
C_6H_6	183.396	−3.54	9.508	0.00
$C_7H_7^+$	264.511	−1.54	12.515	0.00
$C_8H_8^{+2}$	369.700	−0.51	16.017	0.00
$C_8H_8^{-2}$	410.382	−0.98	38.887	0.00
$C_9H_9^-$	549.496	−2.05	48.413	0.00
$C_{10}H_{10}$	720.322	−4.14	59.089	0.00

[a] Sum of squares. See footnote 2. The origin of the coordinate system for each molecule is in the molecular plane of the n-fold axis.

[b] v_{max} is the most positive eigenvalue of the second derivative matrix. See footnote 3.

where ϕ_1 is the p_z orbital on the ith carbon atom and the N's are the normalization constants. These CMO's are transformed into a set of equivalent LMO's, χ, by the following unitary three-orbital transformation, $U(\theta)$:

$$U(\theta)=\begin{bmatrix} \frac{1}{\sqrt{3}} & \sqrt{2/3}\cos\theta & \sqrt{2/3}\sin\theta \\ \frac{1}{\sqrt{3}} & -\sqrt{2/3}\left(\frac{\sqrt{3}}{2}\sin\theta+1/2\cos\theta\right) & \sqrt{2/3}\left(\frac{\sqrt{3}}{2}\cos\theta-1/2\sin\theta\right) \\ \frac{1}{\sqrt{3}} & -\sqrt{2/3}\left(-\frac{\sqrt{3}}{2}\sin\theta+1/2\cos\theta\right) & -\sqrt{2/3}\left(\frac{\sqrt{3}}{2}\cos\theta+1/2\sin\theta\right) \end{bmatrix} \tag{2}$$

When θ is 0° or 60° we obtain a set of three equivalent three-center LMO's which are given for $\theta=0°$ in Eq. 3a (here we have neglected overlap in the normalization constants, N)

$$\begin{aligned} \chi_{2-1-6}&=\frac{1}{3\sqrt{2}}(3\phi_1+2\phi_2+2\phi_6-\phi_4) \\ \chi_{2-3-4}&=\frac{1}{3\sqrt{2}}(3\phi_3+2\phi_2+2\phi_4-\phi_6) \\ \chi_{4-5-6}&=\frac{1}{3\sqrt{2}}(3\phi_5+2\phi_4+2\phi_6-\phi_2) \end{aligned} \tag{3a}$$

or schematically

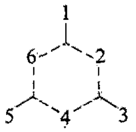

(3b)

When θ is 30° or 90° we obtain Kekulé structures. The orbitals for $\theta=30°$ are given in Eq. 4a

$$\chi_{1-2}=\frac{1}{\sqrt{6}}\left[\left(1+\frac{1}{\sqrt{3}}\right)(\phi_1+\phi_2)+\frac{1}{\sqrt{3}}(\phi_3+\phi_6)+\left(\frac{1}{\sqrt{3}}-1\right)(\phi_4+\phi_5)\right]$$

$$\chi_{3-4}=\frac{1}{\sqrt{6}}\left[\left(1+\frac{1}{\sqrt{3}}\right)(\phi_3+\phi_4)+\frac{1}{\sqrt{3}}(\phi_2+\phi_5)+\left(\frac{1}{\sqrt{3}}-1\right)(\phi_1+\phi_6)\right] \quad (4a)$$

$$\chi_{5-6}=\frac{1}{\sqrt{6}}\left[\left(1+\frac{1}{\sqrt{3}}\right)(\phi_5+\phi_6)+\frac{1}{\sqrt{3}}(\phi_1+\phi_4)+\left(\frac{1}{\sqrt{3}}-1\right)(\phi_2+\phi_3)\right]$$

or schematically

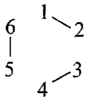

(4b)

Furthermore, it can be shown (see Appendix) using symmetry arguments that the SOS is independent of θ; there are, therefore, an infinite number of sets of equivalent LMO's, $\bar{\chi}=U(\theta)\bar{\psi}$, corresponding to a plateau on the SOS surface. Two limiting structures are given in Eqs. 3 and 4. The flatness of the surface is also reflected by the highest eigenvalues of zero obtained from the second derivative test when only π electrons are included (Table 2). These symmetry arguments can easily be extended to the other $(4n+2)$ π-electron monocyclic systems treated in this paper. Indeed, we find that the π-orbital localizations for all of these molecules are indeterminant as judged by the second-derivative test.

4. Localized Molecular Orbitals: Results

We now discuss the complete electron localizations and compare them with the results based upon π electrons only. For $C_4H_4^{-2}$, the complete localization yields two formally different pairs of carbon atoms. The C atoms in one pair participate in five bonds each: two non-polar τ bonds[4] to one adjacent carbon, two polarized τ bonds to the other adjacent carbon and a σ C–H bond. The non-polar τ bonds which connect this pair of carbons are similar to those in ethylene. The second pair of carbons participate in 4 bonds each: two polar τ bonds, a σ C–C bond and a σ C–H bond. In addition to structure A, there are three other symmetry related structures for C_4H_4 on the complete SOS surface; each such structure corresponds to a well resolved peak as judged by the negative $\nu_{\max}$ found in the second derivative test (Table 2). As noted in previous studies of localizations, we do not find σ-π separation in the LMO's.

The π-LMO sets generated from different starting sets of randomized π-orbitals[5] for $C_4H_4^{-2}$ fall in a range between the limiting structures shown in columns B and

---

[4] For example, the τ bonds in ethylene are formed by taking plus and minus combinations of σ and π bonds between the two carbons yielding two equivalent bent τ bonds, one above the molecular plane and one below.

[5] The starting canonical MO's are usually first subjected to a random unitary transformation. Localization uniqueness can then be tested to some extent by repeating the calculation from different sets of starting orbitals.

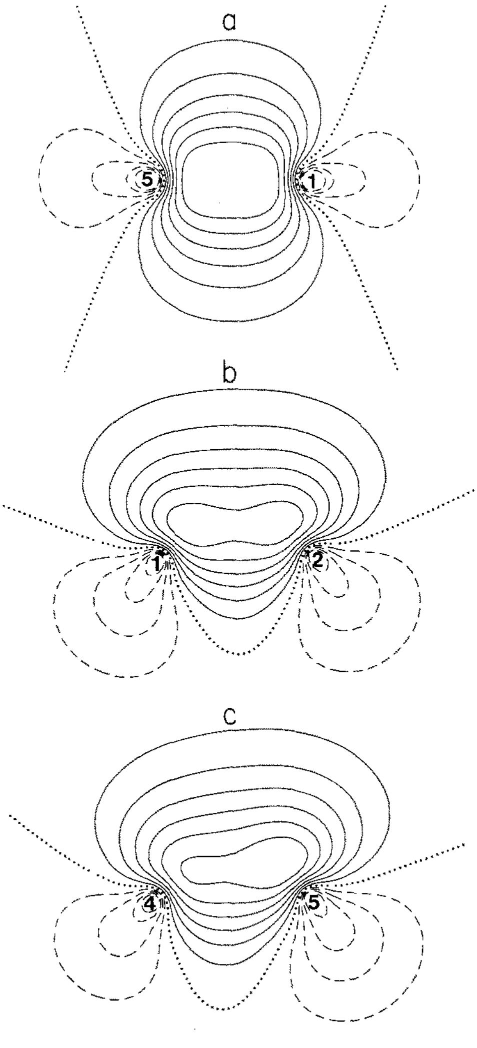

Fig. 3. Contour maps of the wavefunction for the complete LMO's for $C_5H_5^-$. This structure is schematically represented in Fig. 2, column A, with the same numbering. The dotted contour is the nodal line, solid contours are positive and dashed contours are negative. All maps are in a plane perpendicular to the molecular plane. The contour levels are 0.30, 0.25, 0.20, 0.15, 0.10, 0.05, 0.0 (node), −0.05, −0.10 and −0.15 $(e/a.u.^3)^{1/2}$. a) C_1–C_5 σ bond, b) C_1–C_2 symmetric τ bond, c) C_4–C_5 polarized τ bond

C. The structure shown in column B formally resembles the LMO's generated by the complete localization (complete LMO's) while the structure in C corresponds to a lone pair on one carbon that shows substantial delocalization to adjacent centers (or alternatively a weak three center bond) and two polarized bonds to the carbon at the catacorner vertex. As discussed previously, $v_{\max}$ for the second derivative test on π LMO's is zero.

For the complete LMO's in $C_5H_5^-$, we find results similar to those for $C_4H_4^{-2}$ (Fig. 2). One carbon participates in five bonds, as in $C_4H_4^{-2}$; these are four τ

bonds and a σ C–H bond. In Fig. 3 we show contour diagrams for the different types of localized C–C orbitals. Fig. 3a shows one of the C–C σ bonds, which has the striking feature that it is symmetric with respect to the two centers, even though the two centers are formally quite different in the schematic LMO structure. In Fig. 3b we show one of the non-polar τ bonds, where the positive contours are predominantly above the molecular plane and the negative contours are located in two lobes below the plane. A polarized τ bond is shown in Fig. 3c. The polarization is evident from three features: (1) The positive contours are polarized away from the center, C_4, which participates in 5 bonds; (2) the negative lobe on the unique center, C_4, is smaller than that on C_5; (3) the nodal line extends further below the molecular plane than for a normal τ bond (Fig. 3b) and it, too, is asymmetric. We point out that these are the contours for a single structure corresponding to one of five symmetry related maxima on the SOS surface and that each of these structures is less well-determined than those for $C_4H_4^{-2}$ as evidenced by the more positive value of $v_{\max}$ (Table 2).

The π-LMO's for $C_5H_5^-$ in column B are similar to their counterpart complete-LMO's. However, the structure in column C has a symmetric three center bond. In addition, there are an infinite number of localized structures between these limiting cases. In Fig. 4 we show the contours of the π orbitals for the two limiting structures. Fig. 4a illustrates the total π electron density in a plane coplanar to the molecular plane at $z = 1.625$ a.u. and the other contours are also given for this height.

In Fig. 4b and 4c we show the orbitals corresponding to structure C, Fig. 2. As seen in 4b, the three-center bond is symmetric with a node passing between C_5 and C_1 and between C_3 and C_2. The polarized two center C_1–C_5 bond is shown in 4c where the polarization is very apparent from the contours. This orbital is significantly delocalized to C_2. The nodal surface for the two-center bond runs through the atom that is the dominant center in the three-center bond.

The orbitals corresponding to the bonding pattern in column B, Fig. 2, are shown in 4d and 4e. The symmetric two center bond, Fig. 4d, shows some delocalization to the adjacent centers and the node separates C_4 from the remaining centers. The polarized two-center bond, Fig. 4e, is quite delocalized and this is schematically illustrated in Fig. 2b by the dashed arrows.

The LMO's for benzene have been discussed in some detail by England, Salmon and Ruedenberg [13], who considered π-LMO's with the ER criterion from an extended Hückel wavefunction, and by Switkes and Newton [14], who derived complete-LMO's and π-LMO's using the ER criterion from an *ab initio* wavefunction. Here, using the Boys criterion, we find Kekulé structures for the complete localization of the benzene MO's. The Kekulé structures consist of alternating single bonds and pairs of slightly delocalized τ bonds (Fig. 2A). A similar structure was found by Switkes and Newton [14] for the complete localization with the ER criterion. The two Kekulé structures are very well localized as evidenced by the very negative $v_{\max}$ (Table 2). As shown in the previous section, the π-LMO structures based on the Boys criterion form an infinite set ranging between the limiting structures shown in column B (two-center bonds) and column C (three-center bonds) of Fig. 2. These structures are qualitatively similar

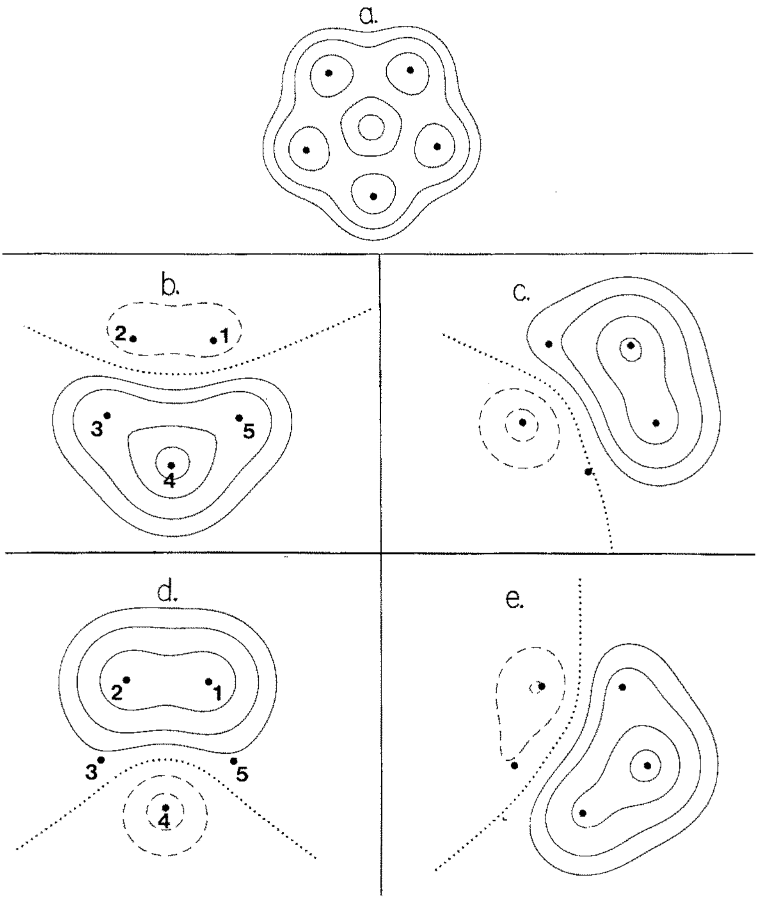

Fig. 4. Contour maps for the π-LMO's of $C_5H_5^-$. All contours are drawn in a plane parallel to the molecular plane and 1.625 a.u. above it. a) Total π-electron density with two electrons in each of the three orbitals. Contours are 0.01, 0.02 and 0.04 e/a.u.^{3}. Note the decrease in density in the center of the molecule. b, c, d and e show contours for the π-LMO's where the numbering permits direct comparison with the schematic π-structures drawn in Fig. 2. The contour representations are described in Fig. 3 with the levels at 0.15, 0.10, 0.05, 0.025, 0.0 (node), −0.025, −0.05 (e/a.u.^{3})$^{1/2}$. b) C_3–C_4–C_5 three center LMO (Fig. 2c). c) C_1–C_5 bond (Fig. 2c). d) C_1–C_2 bond (Fig. 2b). e) C_4–C_5 delocalized bond (Fig. 2b)

to those found by England *et al.* [13]. In our calculations, starting from randomized π-LMO's^5 no preference for any one set of π-LMO's was observed and the indeterminacy of the localization is also reflected by the zero value for the $\nu_{\max}$ of each π-LMO structure. The π-LMO's (Column B) are more delocalized than their τ bond counterparts (Column A). Starting with randomized π-LMO's, we obtained symmetric structures like those in columns B and C of Fig. 2 in only a small fraction of localizations. Actually, most localizations yielded intermediate structures.

The tropylium ion $C_7H_7^+$ exhibits a very interesting localized structure with two pairs of τ bonds and a three-center bond. The remarkable result is that the three-center orbital is almost a pure π orbital with only about 5% s character on the central carbon of the bond. The two sigma bonds beneath the 3-center bond are only slightly bent out of the molecular plane. Thus, an almost complete σ-π separation is found in the localization despite the documented [4] bias of the Boys criterion against such a separation. The second derivative test shows that the structure is still well determined despite the near σ-π separation. For this molecule 14 different but symmetry related structures can be visualized. From a single LMO structure like that depicted in Fig. 2A, seven structures can be generated by cyclic permutations of C atoms. Since the LMO structures are not symmetric with respect to the molecular plane, seven more structures are obtained by reflection through the molecular plane.

The π-localizations again yield a continuous range of structures of which the limiting ones are shown in columns B and C of Fig. 2. Structure B is analogous to the structure obtained from the complete LMO's while structure C has replaced a two-center bond with a three-center bond.

The LMO's for $C_8H_8^{+2}$ are very interesting because in the complete LMO structure, one of the carbons is connected only by single bonds to its flanking carbon neighbors. The three-center bond is almost pure π in character, having less than 1% s character on the central carbon, and the σ bonds beneath this orbital are only slightly bent. As judged by the second derivative test, we find that the complete localization for $C_8H_8^{+2}$ is the least well determined complete localization in this series of compounds. An analysis of the eigenvector corresponding to $v_{\max}$ shows that the major coefficients correspond to mixing the π three-center orbital with the two underlying σ orbitals. This result reflects the bias of the Boys criterion against σ-π separation. We find that the π-LMO's in $C_8H_8^{+2}$ exhibit a range of structures between structure B having two two-center bonds and a three-center bond (analogous to the complete localization) and structure C having two fractional three-center bonds and a two center bond.

We now discuss the localized orbitals for the ten π electron systems beginning with $C_8H_8^{-2}$. For electron rich $C_8H_8^{-2}$ we again find carbon atoms participating in five bonds as in $C_4H_4^{-2}$ and $C_5H_5^-$. Both of these carbon atoms are attached to adjacent carbons by sets of polarized τ-bonds giving a total of four such pairs. Additionally, there is one pair of unpolarized τ bonds (Fig. 2a). For the π-localizations we again find a number of localized structures which correspond to points on a flat SOS plateau as judged by the second derivative tests. These structures include structures B and C (Fig. 2) and a number of intermediate structures. Structure B is formally analogous to the complete LMO structure A.

For $C_9H_9^-$ a new bonding pattern arises in the complete localizations. Three adjacent carbons are bonded to one another by a pair of slightly bent σ-bonds and a three-center bond, and each of the outer carbons in this threesome is in turn bonded to its other nearest neighbor by a pair of τ-bonds. Again we find a partial σ-π separation where the σ bonds are slightly bent and where each of the atomic hybrid orbitals composing the three-center bond has less than 6% s character. However, the structure is quite well resolved as seen by the quite negative $v_{\max}$ (Table 2). In analogy to the results for $C_7H_7^+$, 18 different but symmetry-related structures can be visualized. The π-LMO's show the same features that have been seen previously. We find a limiting set having one three-center bond analogous to the complete LMO structure and another limiting set having fractional three-center bonds.

For $C_{10}H_{10}$, the complete localizations yield the expected Kekulé type of structure having five equivalent pairs of τ-bonds. We find this structure to be the best determined of all of these localizations as judged by the second derivative test (Table 2). For the localizations of π electrons only, we find, as we found in benzene, a limiting structure possessing only two-center LMO's (column B) and another limiting structure having all three-center LMO's. Of course, a number of structures were found between these two extremes.

The π-LMO structures between the limiting structures given in columns B and C show 3-fold and 5-fold symmetry for C_6H_6 and $C_{10}H_{10}$ respectively. In fact, the centroids of π-LMO's for each of the 6 and 10-π electron systems described here are at the vertices of an equilateral triangle or of a regular pentagon, respectively. Localizations from different random starting sets of π MO's simply reorient the triangle or pentagon described by the centroids.

5. Summary

We have discussed the wavefunctions for the monocyclic aromatic $(4n+2)$ rings from the viewpoint of both the canonical and localized MO's. The CMO's are discussed in terms of their eigenvalue spectrum while the LMO's are discussed in terms of their bonding patterns. The LMO's were obtained from both complete localizations and π-only localizations and some interesting effects were observed. The first of these is the discovery of σ-π separation in several of these compounds, even though the Boys criterion is often biased against such separations. We demonstrated for C_6H_6, and found also for the remaining molecules, that the localizations of only π-electrons yield structures corresponding to a plateau on the SOS surface. This indeterminancy of the π-LMO's can be viewed as a corollary of Hückel's famous $4n+2$ rule. We further suggest that there may be a correlation between the highest second derivative eigenvalue obtained from a localization of π electrons only and the "aromaticity" of conjugated and aromatic hydrocarbons. This correlation will be explored more fully in a future publication.

Acknowledgement. We thank the Office of Naval Research for support of this research. We also acknowledge useful discussions with Dr. Thomas A. Halgren and Mr. Leo D. Brown.

Appendix

Application of the unitary transformation, U, (Eq. 2) to the CMOs ψ (Eq. 1) yields a set of localized MO's χ:

$$\chi_a = \frac{1}{\sqrt{3}} [\psi_{A_{2u}} + \sqrt{2}(\cos\theta\psi_{E_{1gy}} + \sin\theta\psi_{E_{1gx}})]$$

$$\chi_b = \frac{1}{\sqrt{3}} \left[\psi_{A_{2u}} + \sqrt{2}\left(\frac{\sqrt{3}}{2}(-\sin\theta\psi_{E_{1gy}} + \cos\theta\psi_{E_{1gx}}) - \frac{1}{2}(\cos\theta\psi_{E_{1gy}} + \sin\theta\psi_{E_{1gx}})\right)\right]$$

$$\chi_c = \frac{1}{\sqrt{3}}\left[\psi_{A_{2u}} - \sqrt{2}\left(\frac{\sqrt{3}}{2}(-\sin\theta\psi_{E_{1gy}} + \cos\theta\psi_{E_{1gx}}) + \frac{1}{2}(\cos\theta\psi_{E_{1gy}} + \sin\theta\psi_{E_{1gx}})\right)\right]$$

Expansion of $\bar{r}_{aa} = \langle\chi_a|\bar{r}|\chi_a\rangle$, $\bar{r}_{bb}$ and $\bar{r}_{cc}$ in terms of dipole moment integrals over the CMO basis yields a large number of terms many of which vanish because of symmetry. For example, in D_{6h} where z transforms as A_{2u} and (x, y) as E_{1u}, $\langle\psi_{A_{2u}}|\bar{r}|\psi_{A_{2u}}\rangle$ vanishes because the direct products $A_{2u} \times A_{2u} \times A_{2u}$ and $A_{2u} \times E_{1u} \times A_{2u}$ do not contain the A_{1_g} representation. In fact, symmetry arguments lead to the conclusion that all dipole moment integrals over the CMOs vanish except

$$\langle\psi_{A_{2u}}|\bar{r}|\psi_{E_{1gy}}\rangle = \langle\psi_{A_{2u}}|x|\psi_{E_{1gy}}\rangle\, \mathbf{x} = I\mathbf{x}$$

and

$$\langle\psi_{A_{2u}}|\bar{r}|\psi_{E_{1gx}}\rangle = \langle\psi_{A_{2u}}|y|\psi_{E_{1gx}}\rangle\, \mathbf{y} = I\mathbf{y}$$

where $\mathbf{x}$ and $\mathbf{y}$ are unit vectors along the x and y axes.
Thus,

$$\bar{r}_{aa} = \langle\chi_a|\bar{r}|\chi_a\rangle = \tfrac{1}{3}(2\sqrt{2}(\cos\theta(I)\mathbf{x} + \sin\theta(I)\mathbf{y}))$$

and

$$\bar{r}^2_{aa} = \tfrac{8}{9}(\cos^2\theta(I)^2 + \sin^2\theta(I)^2) = (8/9)I^2$$

Similarly,

$$\bar{r}^2_{bb} = \bar{r}^2_{cc} = (8/9)I^2$$

so that

$$\mathrm{SOS}(\chi) = \bar{r}^2_{aa} + \bar{r}^2_{bb} + \bar{r}^2_{cc} = (8/3)I^2$$

and the SOS (χ) is independent of the rotation angle θ.

The above proof holds for Boys LMO's. A similar indeterminacy in the ER localized π-LMO's of benzene has been demonstrated by Edmiston and Ruedenberg [15]. A more generalized discussion of continuous degeneracy of ER localized MO's has been presented by England [16]. Although England excludes D_{4h} and C_{4v} as symmetry groups where continuous degeneracy may occur, we find that the Boys LMO's for $C_4H_4^=$ (D_{4h}) are "continuously" degenerate. Furthermore, a Boys localization on B_5H_9 (C_{4v}) also shows a set of "continuously" degenerate LMO's [4].

References

1. Hall,J.H., Dixon,D.A., Kleier,D.A., Halgren,T.A., Brown,L.D., Lipscomb,W.N.: J. Am. Chem. Soc., **97**, 4202 (1975)
2. Edmiston,C., Ruedenberg,K.: Rev. Mod. Phys. **35**, 457 (1963)
3. (a) Boys,S.F.: Rev. Mod. Phys. **32**, 306 (1960), (b) Boys,S.F., in: Quantum Theory of Atoms, Molecules and the Solid State, Löwdin P.O. Ed. 253. New York: Academic Press 1966
4. Kleier,D.A., Halgren,T.A., Hall,J.H., Lipscomb,W.N.: J. Chem. Phys. **61**, 3905 (1974)
5. (a) Lipscomb,W.N.: Accts. Chem. Res. **6**, 257 (1973) and references therein
   (b) Dixon,D.A., Kleier,D.A., Halgren,T.A., Lipscomb,W.N.: J. Am. Chem. Soc. **96**, 2293 (1974)
   (c) Dixon,D.A., Hall,J.H., Kleier,D.A., Halgren,T.A., Lipscomb,W.N.: to be published.
6. Dixon,D.A., Kleier,D.A., Halgren,T.A., Lipscomb,W.N.: to be published
7. Kleier,D.A., Dixon,D.A., Lipscomb,W.N.: to be published
8. Kleier,D.A., Hall, J.H., Halgren,T.A.: Proc. Natl. Acad. Sci. U.S. **71**, 2265 (1974)
9. Switkes,E., Lipscomb,W.N., Newton,M.D.: J. Am. Chem. Soc. **92**, 3847 (1970)
10. Halgren,T.A., Lipscomb,W.N.: J. Chem. Phys. **58**, 1569 (1973)
11. (a) Stevens,R.M., Switkes,E., Laws,E.A., Lipscomb,W.N.: J. Am. Chem. Soc. **93**, 2603 (1971); (b) Lindholm,E., Jonsson,B.Ö.: Chem. Phys. Letters **1**, 501 (1967)
12. (a) Hall,J.H., Marynick,D.S., Lipscomb,W.N.: J. Am. Chem. Soc. **96**, 770 (1974), (b) Dixon,D.A.: unpublished results

13. England,W., Salmon,L.S., Ruedenberg,K.: Fortschr. Chem. Forsch. **23**, 31 (1971)
14. Newton,M.D., Switkes,E.: J. Chem. Phys. **54**, 3170 (1971)
15. Edmiston,C., Ruedenberg,K., in: Quantum theory of atoms molecules and the solid state, P.O. Löwdin (Ed.), p. 263. New York: Academic Press 1966
16. England,W.: Intern. J. Quantum Chem. **5**, 683 (1971)

Dr. D.A. Kleier
Department of Chemistry
Harvard University
Cambridge, Ma. 02138
USA